frontiers
in Earth Science

ORIGINAL RESEARCH
published: 03 December 2020
doi: 10.3389/feart.2020.591711

A Systematic Assessment of Stable Sr Isotopic Compositions of Vent Fluids in Arc/Back-Arc Hydrothermal Systems: Effects of Host Rock Type, Phase Separation, and Overlying Sediment

Toshihiro Yoshimura[1]*, Shigeyuki Wakaki[2], Tsuyoshi Ishikawa[2], Toshitaka Gamo[3], Daisuke Araoka[4], Naohiko Ohkouchi[1] and Hodaka Kawahata[3]

[1]Biogeochemistry Research Center, Japan Agency for Marine-Earth Science and Technology, Yokosuka, Japan, [2]Kochi Institute for Core Sample Research, Japan Agency for Marine-Earth Science and Technology, Nankoku, Japan, [3]Atmosphere and Ocean Research Institute, The University of Tokyo, Kashiwa, Japan, [4]Geological Survey of Japan, National Institute of Advanced Industrial Science and Technology, Tsukuba, Japan

Edited by:
Julia Ribeiro,
Chinese Academy of Sciences, China

Reviewed by:
Aiguo Dong,
China University of Geosciences, China
Xianrong Zhang,
Qingdao Institute of Marine Geology (QIMG), China

***Correspondence:**
Toshihiro Yoshimura
yoshimurat@jamstec.go.jp

Specialty section:
This article was submitted to Geochemistry,
a section of the journal
Frontiers in Earth Science

Received: *05 August 2020*
Accepted: *09 November 2020*
Published: *03 December 2020*

Citation:
Yoshimura T, Wakaki S, Ishikawa T, Gamo T, Araoka D, Ohkouchi N and Kawahata H (2020) A Systematic Assessment of Stable Sr Isotopic Compositions of Vent Fluids in Arc/Back-Arc Hydrothermal Systems: Effects of Host Rock Type, Phase Separation, and Overlying Sediment. Front. Earth Sci. 8:591711. doi: 10.3389/feart.2020.591711

Variations in the stable isotopic composition of seawater Sr (δ^{88}Sr) is a new tool for estimating the rates of global carbonate sedimentation over geologic time, yet the isotope compositions of the major sources and sinks of Sr to the world oceans are still in need of further constraint. We report δ^{88}Sr values of vent fluids from arc/back-arc seafloor hydrothermal systems in the western Pacific. In the sediment-starved hydrothermal fields of the Manus Basin, Izu-Bonin Arc, and Mariana Trough, the δ^{88}Sr values of end-member fluids for each site showed little variation (0.29–0.30‰) and were close to the average value of oceanic volcanic rocks, reflecting dissolved Sr sourced from host rocks. Chlorine-depleted fluids from phase-separated hydrothermal systems in the North Fiji Basin had the end-member δ^{88}Sr values of 0.26, 0.28, and 0.29‰. Thus, both sediment-starved and phase-separated vent fluids had the end-member δ^{88}Sr values indistinguishable from or very close to the range of oceanic volcanic rocks. Therefore, the δ^{88}Sr compositions in these hydrothermal sites are controlled predominantly by Sr sourced from host rock with a small influence from secondary mineral precipitation/re-dissolution. Fluids from the sediment-hosted hydrothermal fields of the Okinawa Trough, however, were characterized by low δ^{88}Sr values of approximately 0.22‰ and high ^{87}Sr/^{86}Sr ratios, indicating interactions with sedimentary carbonates. As for the modern oceanic δ^{88}Sr budget, the sediment-hosted sites lower the global hydrothermal δ^{88}Sr. Since both sediment-starved and -hosted hydrothermal systems provide a long-term control on the global Sr cycle, the end-member δ^{88}Sr value is an important constraint on the evolution of Sr cycling in past oceans.

Keywords: strontium, isotopes, arc, back-arc, convergent margin, hydrothermal vent fluid

INTRODUCTION

Seafloor hydrothermal systems play an important role in chemical and thermal fluxes to the ocean, which impact the evolution of ocean chemistry, climate, and life throughout geologic time (Elderfield and Schultz, 1996; Hardie, 1996). The concentration of Sr^{2+} in seawater is 89 μM, the fifth most abundant cation in seawater, with a mean residence time of about 2.5 million years (Hodell et al., 1990). Strontium inputs from hydrothermal systems have played an important role in past changes of seawater $^{87}Sr/^{86}Sr$ values, accounting for approximately 5% of total input fluxes with end-member $^{87}Sr/^{86}Sr$ values of 0.703–0.704 (Pearce et al., 2015a). These changes in the $^{87}Sr/^{86}Sr$ value of seawater have been used to elucidate the relative intensities of continental weathering and hydrothermal alteration of oceanic crust over time (DePaolo and Ingram, 1985; Hodell et al., 1990; Raymo and Ruddiman, 1992; Veizer et al., 1999; McArthur et al., 2001).

The combined use of radiogenic ($^{87}Sr/^{86}Sr$) and stable isotopic ratios ($^{88}Sr/^{86}Sr$, denoted by $\delta^{88}Sr$) is a novel approach that is useful for identifying differences in Sr sources and processes involving chemical reactions in the Earth's surface (**Figure 1**; Ohno and Hirata, 2007; Halicz et al., 2008; Ohno et al., 2008; Wei et al., 2013; Neymark et al., 2014; Chao et al., 2015; Andrews et al., 2016; Stevenson et al., 2016; Liu et al., 2017; Shalev et al., 2017). Fractionation of $^{88}Sr/^{86}Sr$, but not of $^{87}Sr/^{86}Sr$, accompanies mineral precipitation and biological uptake (Böhm et al., 2012; Stevenson et al., 2014), and is of importance in understanding isotopic mass balance in Earth's Sr cycle. The utility of the isotopic mass balance of $\delta^{88}Sr$ and $^{87}Sr/^{86}Sr$ for the marine Sr budget has been favorably assessed in studies of both modern and past oceans (Krabbenhöft et al., 2010; Pearce et al., 2015a). Modern seawater is isotopically quite homogeneous in terms of both $\delta^{88}Sr$ and $^{87}Sr/^{86}Sr$, irrespective of area or depth (0.39‰ and 0.70917, Wakaki et al., 2017), and seawater Sr concentrations reflect the balance between contributions from hydrothermal systems, marine diagenesis, chemical weathering of continental rocks to seawater, and carbonate burial. The evolution of the seawater $^{87}Sr/^{86}Sr$ value is determined by the balance of inputs from rivers (approximately 0.713) and hydrothermal systems (0.704), whereas the $\delta^{88}Sr$ record reflects primarily changes in the balance between riverine (0.32‰) and hydrothermal (0.24–0.27‰) inputs (**Figure 1**). The removal of marine biogenic carbonates 0.18–0.24‰ depleted in ^{88}Sr leaves the ocean isotopically heavier than $\delta^{88}Sr$ values of the input fluxes (Krabbenhöft et al., 2010; Pearce et al., 2015a). As a result, $\delta^{88}Sr$ of past seawater varied from 0.25 to 0.60‰ in the Phanerozoic era (Vollstaedt et al., 2014). Strontium inputs from hydrothermal systems play a major role in the $^{87}Sr/^{86}Sr$ flux to the ocean (Elderfield and Schultz, 1996), but the magnitude of Sr isotope fractionation and the compositional variation of the end-member solutions in hydrothermal water-rock reactions must be known for accurate estimation of the global marine Sr input and output fluxes (Krabbenhöft et al., 2010). Strontium uptake and release during oceanic hydrothermal circulation may result in its enrichment in certain isotopes from the recharging seawater; the resolution of this key issue requires further investigation in different types of hydrothermal settings.

Most data reported from Mid-Atlantic Ridge (MAR) hydrothermal vent fluids (Krabbenhöft et al., 2010; Pearce et al., 2015a) lie on the mixing line between seawater and an end-member component with estimated $\delta^{88}Sr$ and $^{87}Sr/^{86}Sr$ values of 0.27‰ and 0.7045, respectively (Krabbenhöft et al., 2010), or 0.24‰ and 0.7037 (Pearce et al., 2015a), respectively. These end-member values are consistent with the reference values of oceanic basalt (about 0.25‰, Halicz et al., 2008; Ohno et al., 2008; Pearce et al., 2015a), although the $^{87}Sr/^{86}Sr$ values are slightly higher than those of fresh mid-ocean ridge basalt (MORB). More recently, the $\delta^{88}Sr$ value of MORB has been suggested to be 0.31 ± 0.05‰ (Amsellem et al., 2018). In some MAR hydrothermal fluids, however, $\delta^{88}Sr$ values are higher than expected from the mixing trend (**Figure 2**), and these higher values are interpreted as a result of isotopic fractionation during hydrothermal mineral precipitation or dissolution (Pearce et al., 2015a). A recent experimental study conducted under high-temperature and high-pressure conditions has shown that in fluid-basalt interactions, ^{88}Sr is preferentially taken up into anhydrite (i.e., greater anhydrite precipitation and re-dissolution result in lower and higher $\delta^{88}Sr$ in the fluid, respectively) and ^{86}Sr is preferentially released as a result of the incongruent dissolution of crystalline basalt (Voigt et al., 2018). It is still uncertain to what degree the variation of $\delta^{88}Sr$ values in hydrothermal systems can be attributed to solute sources or secondary mineral (e.g., anhydrite and calcite veins) formation.

In arc and back-arc basins, the chemical compositions of vent fluids vary more widely than those of vent fluids in sediment-starved hydrothermal sites because of the compositional variation of the host rocks as some are buried by sediments (Volpe et al., 1987). Given the tectonic differences between back-arc rifting and mid-ocean ridge spreading zones, it is essential to fully assess $\delta^{88}Sr$ systematics in arc/back-arc settings. In addition, although phase separation and segregation of vapor and fluid phases greatly affect hydrothermal fluid chemistry in both mid-ocean ridge and arc/back arc settings (Von Damm and Bischoff, 1987), the impact of separation and segregation processes on the $\delta^{88}Sr$ values of hydrothermal fluids has not yet been examined. Finally, as an extreme case, hydrothermal fields of back-arc setting include heavily sediment-covered rift that lacks typical oceanic crust, as represented by the Okinawa Trough (**Figure 3**). Terrigenous materials contained in the overlying sediments have considerably influenced the $^{87}Sr/^{86}Sr$ signatures of the hydrothermal fluids in this region (Chiba et al., 1993; Noguchi et al., 2009; Araoka et al., 2016), and $\delta^{88}Sr$ can be utilized to precisely apportion Sr sources in these sediment-hosted fields, that also impact the oceanic $\delta^{88}Sr$ inventory.

The characteristics of hydrothermal systems in arc/back arc settings are diverse with respect to the presence or absence of marine sediments, host-rock type, phase separation, and temperature of the vent fluids. However, how these factors influence $^{88}Sr/^{86}Sr$ fractionation and variations in the $\delta^{88}Sr$ values of the fluids remains unknown. In this study, we investigated the $^{87}Sr/^{86}Sr$ and $\delta^{88}Sr$ systematics of

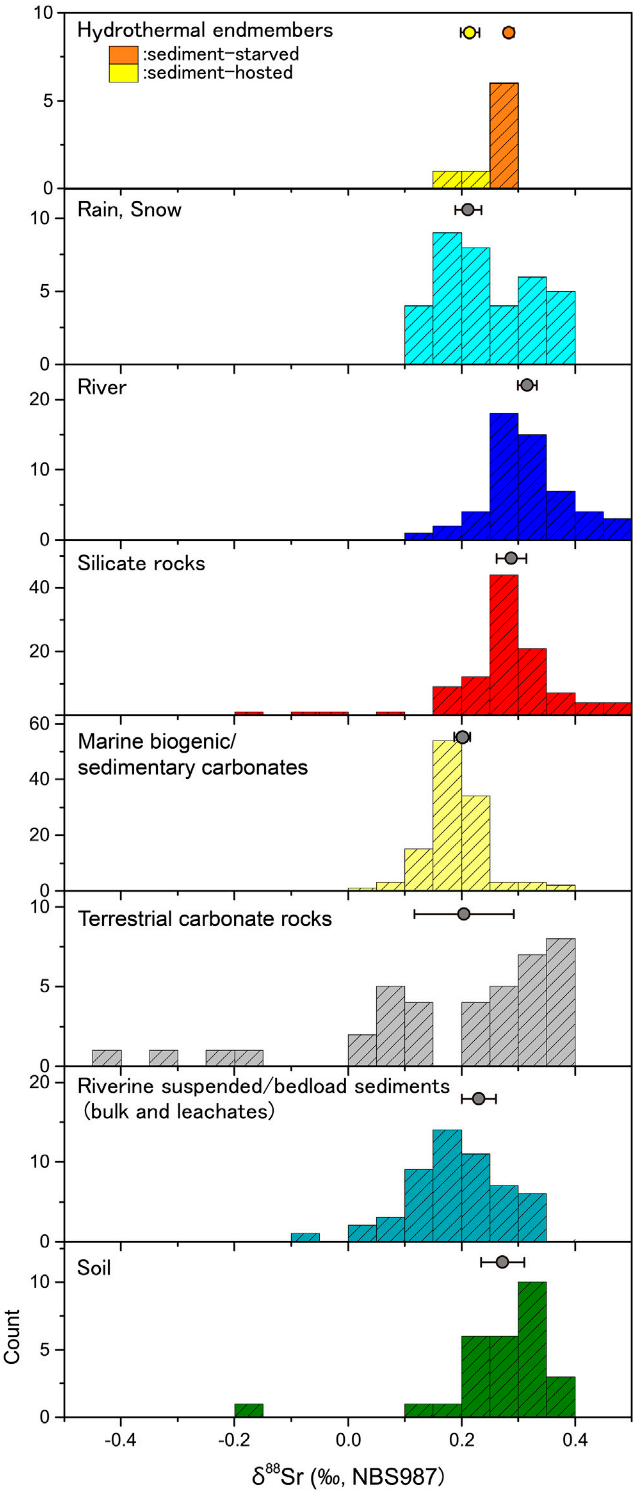

FIGURE 1 | Compilation of δ^{88}Sr values of terrestrial and marine: rain and snow, river water, groundwater, silicate rocks, carbonate rocks, and suspended mixed riverine sediments from glacial catchments. Data are from this study and other published δ^{88}Sr analyses (Ohno and Hirata, 2007; Halicz et al., 2008; Ohno et al., 2008; Rüggeberg et al., 2008; Krabbenhöft et al., 2010; Moynier et al., 2010; Böhm et al., 2012; Charlier et al., 2012; (Continued)

hydrothermal fluids collected from 11 vents in five arc and back-arc hydrothermal systems in the western Pacific. The studied sites, which include both sediment-starved and sediment-hosted sites and cover the large variation in hydrothermal settings described above, provide essential information for comprehensive understanding of Sr geochemistry in hydrothermal systems.

MATERIALS AND METHODS

Geological Settings of Hydrothermal Vents

Hydrothermal vent fluids previously collected from eight sediment-starved sites in the Manus Basin (*n* = 5), Izu-Bonin Arc (*n* = 3), Mariana Trough (*n* = 4), and North Fiji Basin (*n* = 6), and from three sediment-hosted sites in the Okinawa Trough (*n* = 7) are used for this study (**Table 1**; **Figure 3**) (Sakai et al., 1990a; Gamo et al., 1991; Grimaud et al., 1991; Chiba et al., 1993; Ishibashi, 1994; Ishibashi et al., 1994a; Gamo et al., 1997). The chemical variability of the vent fluids as well as hydrothermal mineral deposits of these arc/back-arc hydrothermal systems reflect diversity in geological structures (axial graben, crest of a ridge, seamount, frank of an axial volcano, volcanic depression, and sediment-rich depression) and lithologic types ranging from mafic to felsic rocks (Ishibashi and Urabe, 1995; **Table 2**). The sediment-hosted Okinawa Trough sites are all developed on continental lithosphere, not oceanic lithosphere. According to the estimate of hydrothermal fluid fluxes from the major types of hydrothermal systems (Nakamura and Takai, 2015), the sediment-associated hydrothermal systems yield approximately 10% of the total hydrothermal flux to seawater; the sediment-starved mid-ocean ridge and arc/back-arc hydrothermal systems are estimated to deliver 80% and 10%, respectively. Chemical properties of sediment-starved hydrothermal system are controlled essentially by chemical equilibria between fluids and host rocks, while the hydrothermal fluids in the Okinawa Trough have been shown to interact with terrigenous and biogenic materials (Sakai et al., 1990a; Gamo et al., 1991).

Sediment-Starved Sites (Manus Basin, Izu-Bonin Arc, Mariana Trough, North Fiji Basin)

The Vienna Woods field is located on the central spreading axis in the Manus Basin. This site is hosted in basalt and the chemical characteristics of the vent fluids have been previously reported to be comparable to those of mid-ocean ridge hydrothermal fluids (Lisitsyn et al., 1993; Gamo et al., 1997). The vent fluids of the Pacmanus field, located in the Eastern Manus Volcanic Zone, are characterized by higher K and B concentrations and a lower Ca

FIGURE 1 | Raddatz et al., 2013; Wei et al., 2013; Neymark et al., 2014; Stevenson et al., 2014; Chao et al., 2015; Pearce et al., 2015a, Pearce et al., 2015b; Voigt et al., 2015; Andrews et al., 2016; Fruchter et al., 2016; Stevenson et al., 2016; Liu et al., 2017; Shalev et al., 2017; Amsellem et al., 2018). The circles represent the averages of each material with 95% confidence interval.

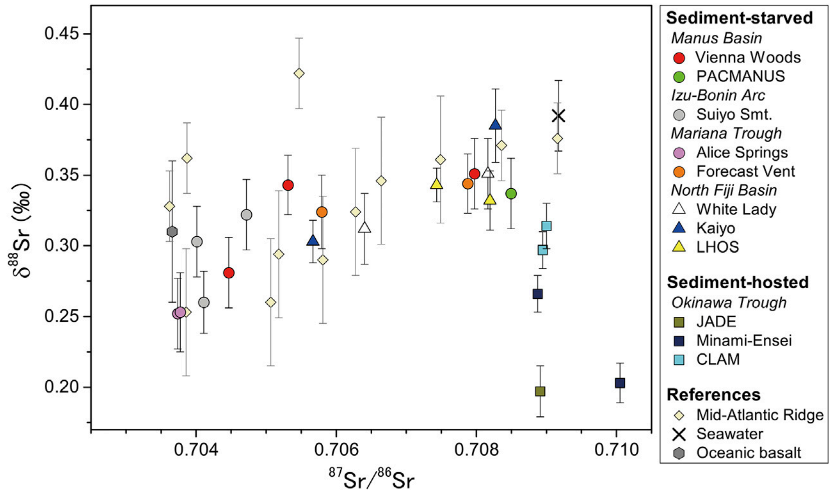

FIGURE 2 | δ^{88}Sr vs. ^{87}Sr/^{86}Sr in hydrothermal waters from western Pacific sites, along with data for the Mid-Atlantic Ridge reported by Krabbenhöft et al. (2010) and Pearce et al. (2015a). Bars represent 2SD errors. Because the internal errors of δ^{88}Sr measurements are generally significantly small compared with long-term external reproducibility, reference data are plotted with the long-term reproducibility of each laboratory: 0.025‰ (n = 33) from Pearce et al. (2015a) and 0.044‰ (n = 90) from Krabbenhöft et al. (2009).

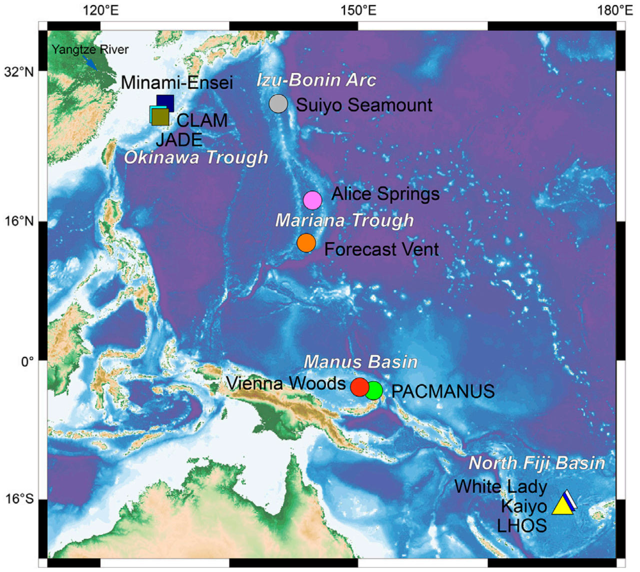

FIGURE 3 | Map showing the sampling site locations. Circles, triangles, and squares represent sediment-starved, phase-separated, and sediment-hosted hydrothermal vents, respectively.

concentration compared with the Vienna Woods fluids, reflecting their interaction with dacitic host rocks (Yamaoka et al., 2015).

The Suiyo Seamount is a dacitic submarine volcano along the volcanic front of the Izu-Bonin Arc. Its fluids are enriched in Ca and Sr, as well as in gaseous CO_2, compared with the fluids from the mid-ocean ridge site (Ishibashi, 1994; Tsunogai et al., 1994).

The Mariana Trough is an actively spreading back-arc basin behind the Mariana Arc. The Alice Springs field is located on the flank of an axial basaltic andesite volcano in the mid-Mariana Trough. Clear, low-temperature (202°C) vent fluids were collected from an anhydrite chimney in the Forecast Vent field at the summit of a seamount in the southern Mariana Trough (Gamo et al., 1994).

The White Lady, Kaiyo, and LHOS sites in the North Fiji Basin have low chlorinity, suggesting segregation of vapor-rich phases (Grimaud et al., 1991). The petrological characteristics of the basalt in the North Fiji Basin are similar to those of normal MORB (N-MORB) but include a regional influence of coexisting oceanic island basalt components (Eissen et al., 1991; Nohara et al., 1994). Fluid samples from the White Lady field were collected from an anhydrite chimney at a topographic high point in the axial graben of the northern-central segment near the triple junction. Two chimneys, Kaiyo and LHOS, are also located in the same segment, 150 m southwest of the White Lady field. The chlorinity of vent fluids in the North Fiji Basin is estimated to be 47–49% that of seawater, suggesting that phase separation occurs beneath the seafloor and that a vapor-rich phase has condensed to form the hydrothermal fluid (Grimaud et al., 1991; Ishibashi et al., 1994b).

Sediment-Hosted Sites (Okinawa Trough)

The Okinawa Trough is a back-arc basin located at the eastern margin of the Eurasian Continent. It is considered to be initiated as continental rifting which commenced since approximately 2 Ma (Sibuet al., 1995). Hydrothermal sites in the Okinawa Trough are hosted in basalt for JADE and rhyolite-andesite for CLAM sites, and accompanied by a thick sediment layer consisting mainly of terrigenous clay derived from the Eurasian Continent (e.g., the Yangtze and Yellow Rivers) and biogenic carbonates (Halbach et al., 2017). For hydrothermal sites in the mid-ocean ridges, the primary fluid source is overlying

TABLE 1 | Sr isotopic ratios and other chemical characteristics of hydrothermal fluid and seawater samples.

	Site	Sr (μmol/kg)	Sr/Ca (mmol/mol)	^{87}Sr/^{86}Sr	δ^{88}Sr (‰)	2sd	Mg (mmol/kg)	Ca (mmol/kg)	SO$_4$ (mmol/kg)	Cl (mmol/kg)
Sediment-starved sites										
303-TS1	Vienna woods	115	6.5	0.707972	0.351	0.025	46.3	17.6	25.3	565
307-1	Vienna woods	187	3.7	0.705312	0.343	0.021	20.3	50.6	11.6	623
307-2	Vienna woods	256	3.4	0.704465	0.281	0.025	2.5	74.7	2.0	687
301-8	Pacmanus	114	8.5	0.706625	—	—	21.0	13.4	11.3	564
304-1	Pacmanus	88	9.2	0.708495	0.337	0.025	42.0	9.5	20.8	545
D630-3	Suiyo seamount	270	—	0.704718	0.322	0.025	17.7	—	—	—
D631-2	Suiyo seamount	307	—	0.704011	0.303	0.025	0.8	—	—	—
D631-6	Suiyo seamount	295	—	0.704109	0.260	0.022	3.7	—	—	—
D154-2	Alice springs	84	3.9	0.703737	0.252	0.025	0.9	21.7	D.L.	582
D154-5	Alice springs	94	4.2	0.703774	0.253	0.028	1.0	22.3	D.L.	548
D182-4	Forecast vent	101	6.0	0.707876	0.344	0.021	43.2	16.8	—	—
D187-2	Forecast vent	147	4.0	0.705794	0.324	0.026	25.3	36.5	—	—
Phase-separated sites										
IST5-2	White lady	42	5.5	0.706405	0.312	0.025	8.6	7.7	4.9	302
IST6-1	White lady	66	8.0	0.708164	0.351	0.025	25.7	8.3	13.3	402
D80-3	Kaiyo	79	8.9	0.708273	0.385	0.026	31.5	8.9	16.7	420
D80-4	Kaiyo	60	6.7	0.705668	0.303	0.015	8.5	9.0	4.5	318
D93-3	LHOS	77	7.7	0.707433	0.343	0.012	24.4	10.0	13.3	401
D93-4	LHOS	80	8.2	0.708194	0.332	0.021	33.5	9.7	18.1	452
Sediment-hosted sites										
D423-3	JADE	180	4.5	0.708911	0.197	0.018	1.0	40.0	D.L.	528
D423-5	JADE	100	7.1	0.709152	—	—	45.2	14.1	24.1	503
D621-5	Minami-ensei	90	5.4	0.708875	0.266	0.013	27.2	16.7	13.7	550
D622-1	Minami-ensei	247	10.8	0.710024	—	—	4.9	22.9	D.L.	550
D622-2	Minami-ensei	252	10.9	0.710051	0.203	0.014	1.4	23.2	D.L.	550
D426-6	CLAM	74	5.2	0.709000	0.314	0.016	39.5	14.3	20.7	—
D427-6	CLAM	91	4.7	0.708948	0.297	0.013	33.4	19.2	—	517
Seawater	—	89	8.7	0.709172	0.392	0.025	52.7	10.3	28.0	546

TABLE 2 | Characteristics of seafloor hydrothermal vents and Sr isotopic end-member compositions.

Site	Type	Host rock	Temp.(°C)	pH at 25°C	Sr end-members		
					Sr (μmol/kg)	^{87}Sr/^{86}Sr	δ^{88}Sr (‰)
Sediment-starved sites							
Vienna woods	Back arc	Basalt	302	4.0–4.5	260	0.70447	0.298
Pacmanus	Back arc	Dacite	268	2.5	126	0.70583	—
Suiyo seamont	Arc	Dacite	311	3.7	320	0.70407	0.291
Alice springs	Back arc	Basalt	280	3.9	89	—	—
Forecast vent	Back arc	Basalt	202	—	196	0.70440	0.288
Phase-separated sites							
White lady	Back arc	Basalt	285	4.7	36	0.70546	0.280
Kaiyo	Back arc	Basalt	291	4.7	56	0.70495	0.290
LHOS	Back arc	Basalt	291	4.7	66	0.70556	0.256
Sediment-hosted sites							
JADE	Back arc	Ryolite-andesite	320	4.7	181	0.70892	0.195
Minami-ensei	Back arc	—	278	4.9–5.1	190	0.70988	0.235
CLAM	Back arc	Basalt	220	5.3	74	0.70909	—

seawater recharged through basaltic outcrops. In contrast, the large reservoir of sedimentary pore water in the thick trough-fill sediments recharges hydrothermal fluids in the sediment-hosted hydrothermal system of the mid-Okinawa Trough (**Figure 4**; Tsuji et al., 2012). Fluid migration driven by thermal advection of the silicic arc volcanism is considered to flow laterally and updip along permeable volcanoclastic sedimentary layers and along basement faults within the crust (Tsuji et al., 2012). These sediment-hosted hydrothermal systems are highly alkaline and enriched in methane derived from thermally altered sedimentary organic matter (Von Damm et al., 1985; Gamo et al., 1991; Kawagucci et al., 2013). The hydrothermal fluids in this area have high alkalinity and are enriched in NH_4^+, CH_4, and CO_2 as a result of interactions with sediments (Sakai et al., 1990a; Sakai et al., 1990b; Gamo et al., 1991; Chiba et al., 1993; Kawagucci et al., 2013).

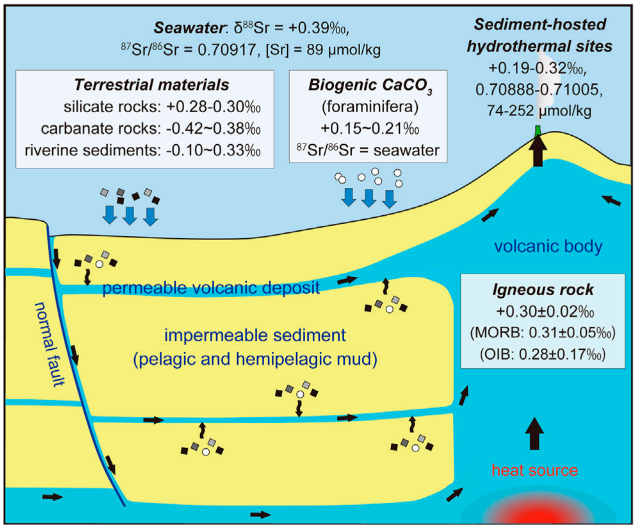

FIGURE 4 | Schematic fluid flow of the hydrothermal system in the sediment-hosted continental back-arc basin of the mid-Okinawa Trough (modified after Tsuji et al., 2012). The primary fluid recharge and migration paths are normal faults and permeable volcanic deposits, and migrate through volcanic body to hydrothermal discharge zones (Tsuji et al., 2012). δ^{88}Sr, ^{87}Sr/^{86}Sr, and [Sr^{2+}] values of terrestrial and marine materials are referenced in **Figure 1**.

The JADE site is a high-temperature (320°C) hydrothermal vent field in the middle Okinawa Trough, and the fluids are emitted from sulfide-sulfate chimneys. The Minami-Ensei knoll is located in a rifting center in the northern Okinawa Trough (Chiba et al., 1993). This knoll is a volcanic complex characterized by a complicated topography of small hills and depressions within a circular rim of 2 km radius. The samples were collected from fragile anhydrite chimneys. The CLAM hydrothermal field is located in a small depression along the eastern Iheya Ridge and is associated with basalt breccia (Ishibashi et al., 1995). Mineralized chimney precipitates of the CLAM field consist mainly of manganoan calcite, rhodochrosite, anhydrite, and amorphous silica (Izawa et al., 1991). At the CLAM site, the end-member fluids contain Mg^{2+} (approximately 20 mM), reflecting a low maximum temperature of 220 °C and suggesting an incomplete water-rock reaction (Sakai et al., 1990b).

Analytical Methods

Hydrothermal fluid samples were filtered, acidified with HNO_3, and stored in polypropylene bottles. Major and trace element concentrations and δ^7Li, δ^{11}B, δ^{26}Mg, ^{87}Sr/^{86}Sr values of the fluid samples have been reported previously (Yamaoka et al., 2015; Araoka et al., 2016; Eom et al., 2020).

δ^{88}Sr and ^{87}Sr/^{86}Sr values of the samples were determined simultaneously using the double-spike technique (Wakaki et al., 2017) in a TRITON thermal ionization mass spectrometer (Thermo Scientific, Germany) at Kochi Core Center, Japan. Two aliquots of each fluid sample, with and without the addition of the ^{84}Sr-^{86}Sr spike, were prepared for Sr isotopic analysis. After chemical separation of Sr by a Sr-Spec resin (Eichrom resin), the Sr sample with a Ta activator was loaded onto a single W filament. The $^{88}Sr^+$ beam intensities were approximately 11 and 4 V for the unspiked and spiked runs, respectively. Peaks for ^{88}Sr, ^{87}Sr, ^{86}Sr, ^{84}Sr, and ^{85}Rb were monitored. The ^{87}Sr/^{86}Sr ratio was measured in the unspiked sample by the conventional internal normalization technique using ^{86}Sr/^{88}Sr = 0.1194 and the exponential law. Stable ^{88}Sr/^{86}Sr ratios were calculated by using the data from the unspiked and spiked runs, and expressed as permil (‰) deviations relative to the NBS-987 standard as:

$$\delta^{88}\mathrm{Sr} = \left\{\left(^{88}\mathrm{Sr}/^{86}\mathrm{Sr}\right)_{\mathrm{sample}}/\left(^{88}\mathrm{Sr}/^{86}\mathrm{Sr}\right)_{\mathrm{NBS-987}} - 1\right\} \times 1{,}000. \quad (1)$$

Repeated analyses of the in-house Sr isotopic reference reagent Wako-9999 (Wakaki et al., 2017) gave δ^{88}Sr = 0.322 ± 0.025‰ (2 SD, $n = 45$). The external error for vent fluid samples was estimated as the 2SD repeatability of multiple SRM-987 analyses during each analytical session (Wakaki et al., 2017) and ranged from ±0.013‰ to ±0.028‰ (**Table 1**). To check the accuracy of the analysis, we analyzed the IAPSO seawater (0.392 ± 0.015‰, 2 SE, $n = 3$) as reference material, and consistent with published values for seawater samples from the Atlantic, Pacific, Indian, and Southern Oceans (Krabbenhöft et al., 2009; Neymark et al., 2014; Stevenson et al., 2014; Vollstaedt et al., 2014; Pearce et al., 2015a). The conventional ^{87}Sr/^{86}Sr ratios obtained by unspiked runs were corrected for a small systematic mass bias to give $^{87}\mathrm{Sr}/^{86}\mathrm{Sr}_{\mathrm{SRM\text{-}987}} = 0.710248$. Typical repeatability of the ^{87}Sr/^{86}Sr ratios was ±0.000005 (2SD). The ^{87}Sr/^{86}Sr values determined in this study were essentially consistent with those previously reported by Araoka et al. (2016). For consistency with the δ^{88}Sr values, we used the newly determined ^{87}Sr/^{86}Sr values in the present analysis.

RESULTS

We examined the relationship between δ^{88}Sr and ^{87}Sr/^{86}Sr in the hydrothermal fluids and compared the result with data for MAR hydrothermal fluids (Krabbenhöft et al., 2010; Pearce et al., 2015a) and MORB (Amsellem et al., 2018) (**Figure 2**; **Table 1**). The samples from sediment-starved (Manus Basin, Izu-Bonin Arc, and Mariana Basin) and phase-separated (North Fiji Basin) sites showed a clear positive correlation between δ^{88}Sr and ^{87}Sr/^{86}Sr (**Figure 2**) and plot right along with the data reported previously by Krabbenhöft et al. (2010) for MAR. All ^{87}Sr/^{86}Sr values of the fluids from the sediment-hosted sites (Okinawa Trough) were distinctly higher than those from the other sites, and the δ^{88}Sr values were distinctly lower. The fluids from sites in the Okinawa Trough had the following characteristics: 1) their ^{87}Sr/^{86}Sr values are similar to or even higher than the seawater value; 2) on the ^{87}Sr/^{86}Sr–δ^{88}Sr scatter plot, they are outliers compared with the trend for sediment-starved sites; and 3) δ^{88}Sr values of fluids from the JADE and

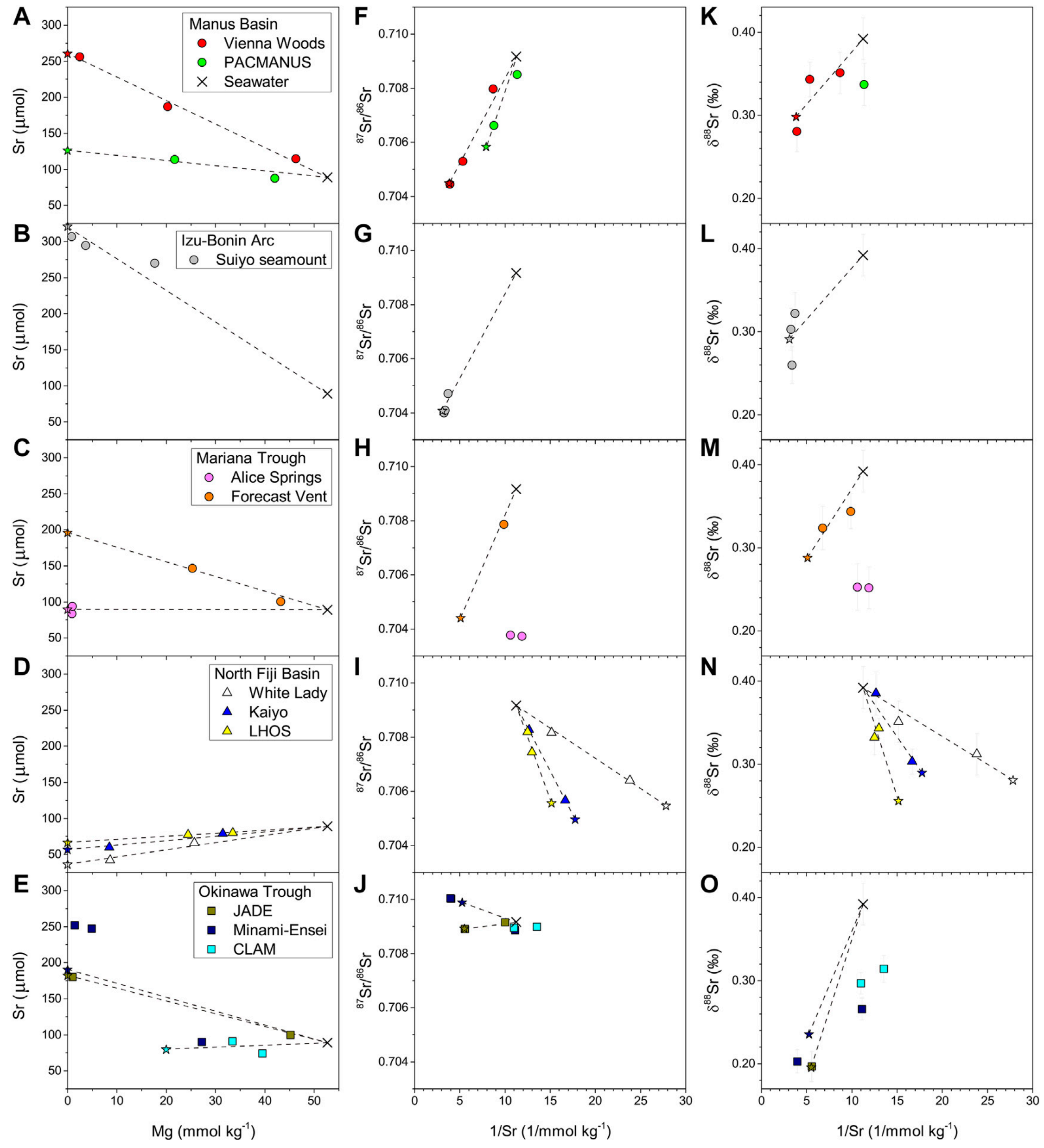

FIGURE 5 | Plots of **(A–E)** [Sr^{2+}] vs. [Mg^{2+}], and **(F–J)** $^{87}Sr/^{86}Sr$ and **(K–O)** $\delta^{88}Sr$ vs. 1/[Sr^{2+}] in hydrothermal fluid samples. End-member elemental and isotopic compositions (stars) for individual vents were estimated by linear regression forced through seawater values (crosses) and by extrapolating the observed Sr-Mg linear regression line to Mg = 0, except at the CLAM site, where it was extrapolated to Mg = 20 mM (Gamo et al., 1991).

Minami-Ensei sites were approximately 0.20‰ or less (**Figure 2**; **Table 1**).

Because hydrothermal fluid samples represent a mixture of seawater and the end-member hydrothermal fluid, previous studies calculated $\delta^{88}Sr$ end-member values by extrapolating Mg/Sr to zero (**Supplementary Figure S1**). This approach is based on the hypothesis that Sr and Mg concentrations are closely coupled through water-rock reactions. However, hydrothermal fluids can experience either a net gain or loss of Sr, compared with the initial seawater concentration, during hydrothermal fluid circulation (Kawagucci et al., 2013), irrespective of whether the Mg concentration is close to zero in the end-member fluid. In this study, the Sr concentrations of the end-member fluid at each site were estimated by extrapolating the observed Sr-Mg linear regression line fitted to the data of two or three samples from each site to Mg = 0 (**Figures 5A–E**). For the CLAM site only, the regression line was extrapolated to an estimated end-member Mg content of 20 mmol/kg (Araoka et al., 2016) based on the observed relatively low maximum temperature of approximately 220 °C (Sakai et al., 1990a; Gamo et al., 1991).

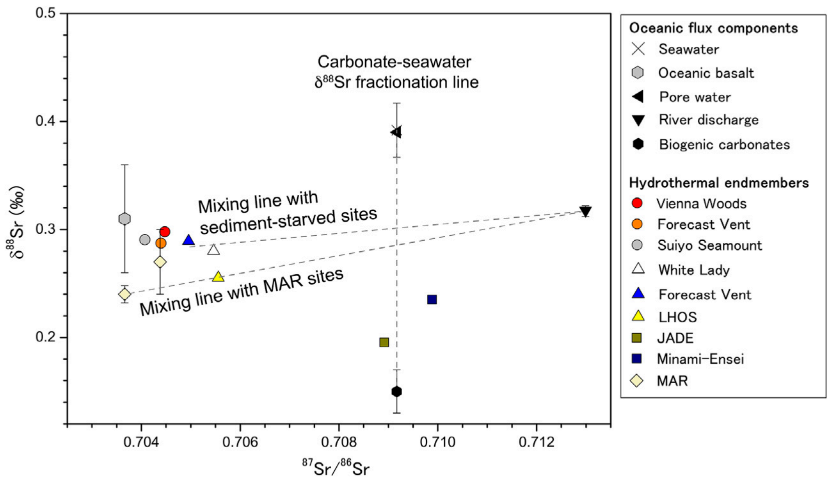

FIGURE 6 | δ^{88}Sr plotted against ^{87}Sr/^{86}Sr for hydrothermal end members of western Pacific hydrothermal vents and for the Mid-Atlantic Ridge (Krabbenhöft et al., 2010; Pearce et al., 2015a) along with major oceanic flux components reported by Pearce et al. (2015a).

At most sites, both ^{87}Sr/^{86}Sr (**Figures 5F–J**) and δ^{88}Sr (**Figures 5K–O**) values were linearly related to 1/Sr; therefore, the end-member Sr isotopic compositions were calculated using the end-member Sr concentrations. All linear regression lines were forced through the seawater end point. Significant correlations were not observed between δ^{88}Sr and 1/Sr in samples from the Pacmanus, Alice Springs, and CLAM sites because these samples had a Sr concentration similar to that of seawater. The estimated end-member compositions are summarized in **Table 2** along with the type of hydrothermal system, host rock, observed maximum temperature, and pH (**Table 2**).

Compared to seawater values (Sr = 89 μmol/kg, δ^{88}Sr = 0.392‰, and ^{87}Sr/^{86}Sr = 0.709, 172), the end-member fluids of the sediment-starved sites were characterized by higher Sr concentrations of up to 320 μmol/kg and lower δ^{88}Sr and ^{87}Sr/^{86}Sr values of 0.29–0.30‰ and 0.7041–0.7058, respectively. Slight differences from the ^{87}Sr/^{86}Sr values reported by Araoka et al. (2016) are because the regression line was forced through the seawater end point. Most Sr isotopic end-member values for samples from the phase-separated sites were similar to those of samples from the sediment-starved sites, but the Sr concentrations were notably lower. The δ^{88}Sr end-member of most sediment-starved sites is in good agreement with MORB composition. The global marine δ^{88}Sr and ^{87}Sr/^{86}Sr fluxes are assessed by an intercept point between 1) a fractionation line between seawater-carbonate and 2) a binary mixing line of hydrothermal-river endmembers (**Figure 6**; Krabbenhöft et al., 2010; Pearce et al., 2015a). The LHOS δ^{88}Sr value (0.26‰) was lower than the values at the sediment-starved and other phase-separated sites. The sediment-hosted sites in the Okinawa Trough exhibited markedly high ^{87}Sr/^{86}Sr (0.7089–0.7099) and low δ^{88}Sr (0.20–0.24‰) values, and Sr concentrations varied greatly among these sites (**Table 2**). The end-member values for the sediment-hosted sites are close to the value of marine biogenic carbonates (δ^{88}Sr = 0.150‰, ^{87}Sr/^{86}Sr = 0.70917) rather than that of igneous rocks (**Figure 6**).

DISCUSSION

Host Rock and Fractionation Controls on δ^{88}Sr in Sediment-Starved Systems

The data obtained in this study provide insights into the control of δ^{88}Sr in end-member fluids associated with hydrothermal systems with varied host rock compositions and with or without phase separation. The Vienna Woods field in the Manus Basin is a basalt-hosted hydrothermal system in MORB-like basaltic rocks (Dril et al., 1997; Gamo et al., 1997). In contrast, the host rocks of the Pacmanus field in the Manus Basin and the Suiyo Seamount site in the Izu-Bonin Arc are arc-type dacitic rocks. The geochemical characteristics of the Mariana Trough basalts reflect a mixing of melts in the source region prior to eruption (Volpe et al., 1987) with abundant CO_2 derived from subducting slab material (Gamo et al., 1997). Among these sites, the dacite-hosted Pacmanus site alone has a high ^{87}Sr/^{86}Sr value of 0.7058. The δ^{88}Sr end-member values at the five sediment-starved sites in these hydrothermal fields are similar at approximately 0.29‰ (**Table 2**). The estimated δ^{88}Sr end-member values are 0.02–0.04‰ higher than those of the MAR reported by Krabbenhöft et al. (2010) and Pearce et al. (2015a). Amsellem et al. (2018) recently demonstrated that igneous processes have a limited effect on ^{88}Sr/^{86}Sr value of MORB and also on ocean island basalts over a wide range of MgO contents. The δ^{88}Sr value of MORB is 0.31 ± 0.05‰, which is close to those of the bulk silicate earth (0.30 ± 0.02‰) and carbonaceous chondrites (0.29 ± 0.06‰) (Amsellem et al., 2018). Regarding different host-rock types, basalts, granites, and andesites have similar average values (Moynier et al., 2010; Charlier et al., 2012; Amsellem et al., 2018). The calculated end-member fluids of the sediment-starved sites (0.284 ± 0.030‰) suggest that δ^{88}Sr is essentially independent of rock type (basalt, dacite) and hydrothermal setting (volcanic front, back-arc basin). Therefore, the δ^{88}Sr values of end-

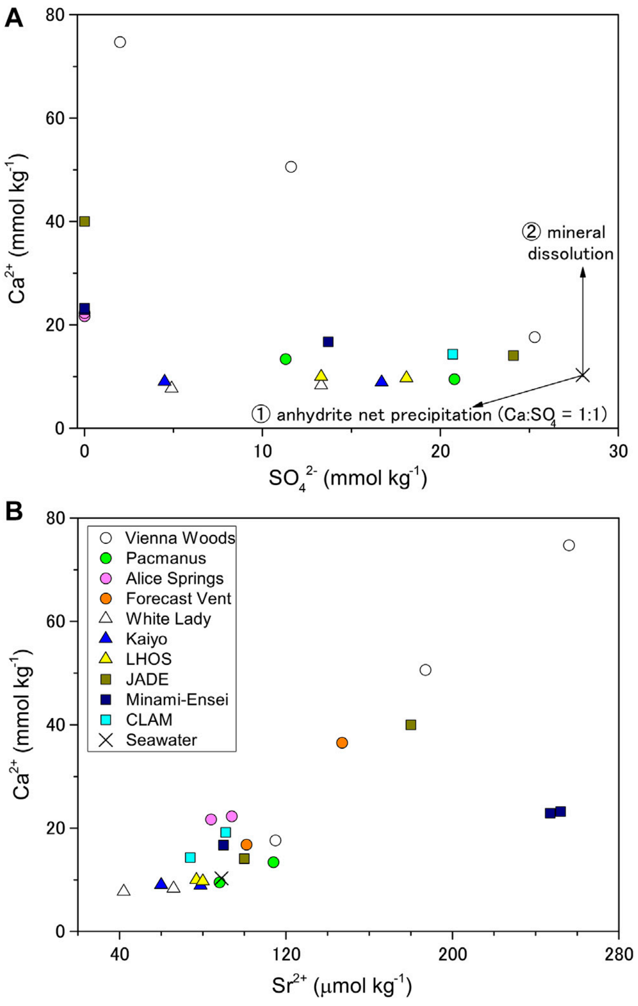

FIGURE 7 | Plots of [Ca^{2+}] vs. **(A)** [SO_4^{2-}] and **(B)** [Sr^{2+}] for the western Pacific hydrothermal vents. Two vectors in the Ca^{2+}-SO_4^{2-} plane explain the expected concentration changes due to anhydrite precipitation and mineral dissolution of host rocks and sediments.

member fluids for each site mainly reflect dissolved Sr sourced from host rocks.

We observed little systematic offset at two phase-separated sites, White Lady and Kaiyo, relative to the sediment-starved sites, which suggests that the phase separation and segregation has minimal impact on hydrothermal δ^{88}Sr values. The three North Fiji Basin sites are all hosted by MORB-like basalt (Ishibashi et al., 1994b; Yamaoka et al., 2015) and have similar physicochemical conditions (**Table 2**) with their δ^{88}Sr values being in the range of oceanic basalt (Amsellem et al., 2018).

The LHOS field in the North Fiji Basin had a slightly lower δ^{88}Sr end-member value (0.26‰) compared with those of the other phase-separated sites. We wish to address the possibility that it is lower due to the impact of anhydrite precipitation/re-dissolution, as well as hydrothermal calcite veins. Voigt et al. (2018) conducted an experiment, demonstrating that the formation of hydrothermal anhydrite and the preferential dissolution of ^{86}Sr-enriched minerals occurs during seawater-basalt reactions at 250°C and 290°C; together, these processes account for 0.07–0.18‰ decrease in the δ^{88}Sr values of fluids after a few months of reaction time between seawater and basaltic materials. Because Sr^{2+} co-precipitation in anhydrite serves as the main Sr sink in hydrothermal reactions, we used Ca^{2+} and SO_4^{2-} concentrations to infer the contributions of rock dissolution and anhydrite precipitation (**Figure 7A**) to the end-member δ^{88}Sr values. The vectors in **Figure 7A** show the directions associated with anhydrite precipitation (a decrease in the 1:1 M ratio) and rock dissolution (predominantly the release of Ca^{2+}) on the scatter diagram of Ca^{2+} and SO_4^{2}. The overall magnitude of the rock dissolution effect relative to the anhydrite precipitation effect was less at phase-separated sites than those of the other sediment-starved sites (**Figure 7A**). An impact of anhydrite precipitation on the lower δ^{88}Sr values of LHOS site was also evaluated using a simple closed/semi-closed type fractionation (**Supplementary Figure S2**). The anhydrite-fluid fractionation factor $\varepsilon_{\text{anhydrite-fluid}}$ of 0.034 ± 0.019‰ (Voigt et al., 2018) was used for calculation. We considered two extreme cases: 1) anhydrite precipitation from recharged seawater (0.392‰), and 2) anhydrite precipitation from end-member fluids of other sediment-starved sites in the North Fiji Basin (0.285‰). In the former case, 98% removal of Sr by anhydrite is necessary to obtain the LHOS end-member of 0.256‰; in the latter case, 58% is necessary. However, Sr concentrations of the LHOS end-member (66 μmol/kg) is about half of that of seawater (89 μmol/kg), and higher than other end-members in the North Fiji Basin (36 μmol/kg for White Lady, 56 μmol/kg for Kaiyo, **Table 2**). Because of the similarity of the end-member δ^{88}Sr values among the sediment-starved sites, Sr co-precipitation with anhydrite cannot by itself account for the lower δ^{88}Sr end-member value at the LHOS site. Therefore, the variation in δ^{88}Sr value of oceanic basalt (0.31 ± 0.05‰, Amsellem et al., 2018) would be an explanation for the lower δ^{88}Sr value of LHOS site. Similar to anhydrite, the impact of Sr co-precipitation within hydrothermal calcite veins is also considered to be negligible, as calculated from the magnitude of Ca depletion observed in the hydrothermal fluids and the partitioning coefficient for Sr to Ca ratios (Rimstidt et al., 1998).

The difference between the flux-weighted marine δ^{88}Sr-^{87}Sr/^{86}Sr input and the intercept value has been attributed to an elevated supply of riverine Sr to the ocean due to post-glacial weathering (**Figure 6**; Krabbenhöft et al., 2010; Pearce et al., 2015a). Our data imply that the mean marine δ^{88}Sr composition of hydrothermal input may be closer to an average oceanic crustal value of approximately 0.30‰ (Amsellem et al., 2018), as it gives a higher intercept δ^{88}Sr value (**Figure 6**).

Influence of Host Sediments on Okinawa Trough Hydrothermal Fluids

The Sr isotopes in the end-member hydrothermal fluids from the sediment-hosted vents in the Okinawa Trough have ^{87}Sr/^{86}Sr values distinctly higher than the other vent (approximately 0.710–0.709 vs. < 0.705, Noguchi et al., 2009) as well as distinctly lower δ^{88}Sr values (approximately 0.22 vs. 0.28‰). The higher ^{87}Sr/^{86}Sr values most likely reflect hydrothermal interaction with the clastic fraction of the host sediments.

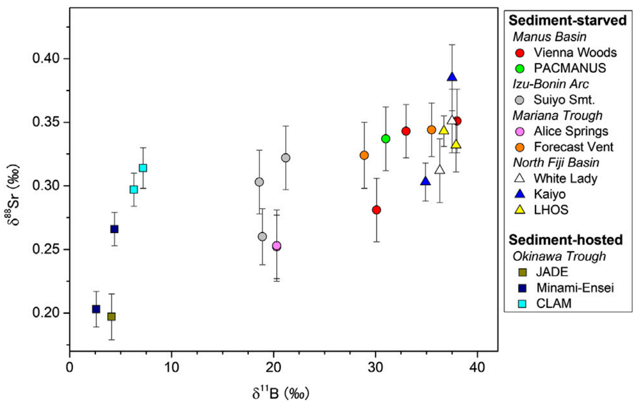

FIGURE 8 | δ^{88}Sr vs. δ^{11}B in hydrothermal waters from western Pacific sites. The boron data were previously reported by Yamaoka et al. (2015).

Unlike the thick sedimentary sequences that overlie basaltic crust on the flanks of mid-ocean ridges, the chemical properties of fluids from sediment-hosted sites strongly reflect contributions of sediment-derived components; e.g., high CH_4 and NH_4 in the fluids (Sakai et al., 1990a; Sakai et al., 1990b; Gamo et al., 1991; Chiba et al., 1993; Kawagucci et al., 2013). These Okinawa Trough samples also have extremely high B and Cs concentrations, derived predominantly from clay minerals, and relatively low δ^{11}B values (Yamaoka et al., 2015). δ^{11}B are characterized by a strong correlation with δ^{88}Sr (R^2 = 0.82, **Figure 8** is readily leached out from the solid phase by fluids at high temperatures (You et al., 1994; Yamaoka et al., 2015), suggesting extensive water-sediment interaction in the Okinawa Trough. The hydrothermal system in the Okinawa Trough is sourced from complex migration networks for recharge and discharge via normal faults that extend from the seafloor to crustal basement and pore fluids in sediments of a thickness of about a few km (**Figure 4**; Tsuji et al., 2012).

The δ^{88}Sr of a wide range of silicate rocks show nearly identical values around 0.28–0.30‰ (Moynier et al., 2010; Amsellem et al., 2018). The only solid-phase reservoir with distinctly lower δ^{88}Sr values are carbonates, suggesting the lower δ^{88}Sr in the Okinawa hydrothermal fluids likely reflects Sr inputs from carbonates in the host sediments (**Figures 1**,**6**). Some continental carbonate rocks are more depleted in ^{88}Sr down to δ^{88}Sr of −0.4‰ (**Figure 1**; Ohno et al., 2008). Potential sources of Sr that can account for the decrease in the δ^{88}Sr are marine biogenic carbonate (0.15–0.23‰, Krabbenhöft et al., 2010; Böhm et al., 2012; Stevenson et al., 2014; Pearce et al., 2015a; Voigt et al., 2015, ^{87}Sr/^{86}Sr = 0.7089–0.7092 for Late Miocene to Holocene biogenic $CaCO_3$, McArthur et al., 2001) in trough-filling hemipelagic sediments. In turn, this suggests that the actual ^{87}Sr/^{86}Sr value of the detrital component in sediment is higher than the measured >0.709 originated from catchments of the Yangtze and Yellow Rivers. The sediment-hosted vent fluids are affected by variable contributions from sedimentary silicate and carbonate sources. The combined use of ^{87}Sr/^{86}Sr and δ^{88}Sr demonstrated that the main Sr sources in overlying sediments are carbonates.

Despite the similar sedimentary origins of D621-5, D622-1 and D622-2, two vents at the Minami-Ensei site, the chemical data differ considerably between them (**Table 1**). The chemical characteristics of the D622-2 vent fluid, including the end member Sr concentration of 252 μM, are comparable to those of the vent fluids of Minami-Ensei Knoll reported by Kawaguchi et al. (2013). Although D621-5 is chemically similar to the other sediment-hosted samples, D622-2 exhibited higher Sr/Ca ratios and ^{87}Sr/^{86}Sr values that were trend outliers. Previous studies have reported that the fluid/sediment mass ratio during interactions of circulating hydrothermal fluids with terrigenous sediments determines the leaching of fixed and adsorbed trace elements from sediments (Yamaoka et al., 2015; Araoka et al., 2016). Therefore, inter-vent variability is also related to heterogeneity of the sediments (such as relative abundance of hemipelagic sediments to volcanic deposits) and the scales of subseafloor hydrothermal fluid flow structures at sediment-hosted sites.

CONCLUSION

We investigated δ^{88}Sr in submarine vent fluids from arc and back-arc hydrothermal systems in the western Pacific. The important observation of this study is that the end-member δ^{88}Sr values (0.256–0.298‰, calculated by extrapolating the linear regression line fitted to data from two or three samples from each site to a Mg concentration of zero) are similar to the average value of oceanic volcanic rocks, about 0.28–0.31‰ (Amsellem et al., 2018). This result confirms the utility of the δ^{88}Sr mass balance for past changes in the marine carbonate system (Krabbenhöft et al., 2010; Vollstaedt et al., 2014; Pearce et al., 2015a), and supports the view that hydrothermal end-member in sediment-starved hydrothermal systems is probably a unique δ^{88}Sr value through geologic time because of the similarity and homogeneity of stable Sr isotopes in between igneous rocks as well as carbonaceous chondrites (Amsellem et al., 2018). The decreased δ^{88}Sr values, as low as 0.20‰, accompanied by higher ^{87}Sr/^{86}Sr, in vent fluids of the sediment-hosted sites are linked to the release of Sr from sedimentary materials, that we find to be sensitive to the extent of mixing between the different sources and sinks of sedimentary Sr phases. A global average of hydrothermal δ^{88}Sr value would be reassessed with taking into account these data and other representative hydrothermal system, such as the East Pacific Rise.

DATA AVAILABILITY STATEMENT

The original contributions presented in the study are included in the article/**Supplementary Material**, further inquiries can be directed to the corresponding author.

AUTHOR CONTRIBUTIONS

TY, SW, and HK contributed to conception of the study. Samples were collected by TG. TY, SW, and TI performed the isotopic analysis. DA performed the trace metal analysis. TY wrote the first draft of the manuscript with input from NO, TI, and SW. SW wrote the analytical sections of the manuscript. All authors contributed to manuscript revision, read, and approved the submitted version.

FUNDING

This work was undertaken with the support of Japan Society for the Promotion of Science (JSPS) to TY (no. 16H05883, 19K21908), to SW (no. 18K03814) and to TG (no. 16H02701).

ACKNOWLEDGMENTS

We thank Kazuya Nagaishi and Tatsuya Kawai of Marine Work Japan for their support during the analysis. The suggestions of Thomas M. Blattmann greatly improved the language. The comments of the reviewers are gratefully acknowledged.

SUPPLEMENTARY MATERIAL

The Supplementary Material for this article can be found online at: https://www.frontiersin.org/articles/10.3389/feart.2020.591711/full#supplementary-material

REFERENCES

Amsellem, E., Moynier, F., Day, J. M. D., Moreira, M., Puchtel, I. S., and Teng, F.-Z. (2018). The stable strontium isotopic composition of ocean island basalts, mid-ocean ridge basalts, and komatiites. *Chem. Geol.* 483, 595–602. doi:10.1016/j.chemgeo.2018.03.030

Andrews, M. G., Jacobson, A. D., Lehn, G. O., Horton, T. W., and Craw, D. (2016). Radiogenic and stable Sr isotope ratios (87 Sr/86 Sr, δ 88/86 Sr) as tracers of riverine cation sources and biogeochemical cycling in the Milford Sound region of Fiordland, New Zealand. *Geochem. Cosmochim. Acta.* 173, 284–303. doi:10.1016/j.gca.2015.10.005

Araoka, D., Nishio, Y., Gamo, T., Yamaoka, K., and Kawahata, H. (2016). Lithium isotopic systematics of submarine vent fluids from arc and back-arc hydrothermal systems in the western Pacific. *Geochem. Geophys. Geosyst.* 17 (10), 3835–3853. doi:10.1002/2016gc006355

Böhm, F., Eisenhauer, A., Tang, J., Dietzel, M., Krabbenhöft, A., Kisakürek, B., et al. (2012). Strontium isotope fractionation of planktic foraminifera and inorganic calcite. *Geochem. Cosmochim. Acta.* 93, 300–314. doi:10.1016/j.gca.2012.04.038

Chao, H.-C., You, C.-F., Liu, H.-C., and Chung, C.-H. (2015). Evidence for stable Sr isotope fractionation by silicate weathering in a small sedimentary watershed in southwestern Taiwan. *Geochem. Cosmochim. Acta.* 165, 324–341. doi:10.1016/j.gca.2015.06.006

Charlier, B. L. A., Nowell, G. M., Parkinson, I. J., Kelley, S. P., Pearson, D. G., and Burton, K. W. (2012). High temperature strontium stable isotope behaviour in the early solar system and planetary bodies. *Earth Planet Sci. Lett.* 329-330, 31–40. doi:10.1016/j.epsl.2012.02.008

Chiba, H., Nakashima, K., Gamo, T., Ishibashi, J., Tsunogai, U., and Sakai, H. (1993). Hydrothermal activity at the Minami-Ensei Knoll, Okinawa Trough: chemical characteristics of hydrothermal solutions. *Proc. JAMSTEC Symp. Deep Sea Res.*

DePaolo, D. J., and Ingram, B. L. (1985). High-resolution stratigraphy with strontium isotopes. *Science* 227 (4689), 938–941. doi:10.1126/science.227.4689.938

Dril, S. I., Kuzmin, M. I., Tsipukova, S. S., and Zonenshain, L. P. (1997). Geochemistry of basalts from the western Woodlark, Lau and Manus basins: implications for their petrogenesis and source rock compositions. *Mar. Geol.* 142 (1–4), 57–83. doi:10.1016/s0025-3227(97)00041-8

Eissen, J.-P., Lefevre, C., Maillet, P., Morvan, G., and Nohara, M. (1991). Petrology and geochemistry of the central North Fiji basin spreading centre (southwest pacific) between 16 S and 22 S. *Mar. Geol.* 98, 2–4. doi:10.1016/0025-3227(91)90104-c

Elderfield, H., and Schultz, A. (1996). Mid-ocean ridge hydrothermal fluxes and the chemical composition of the ocean. *Annu. Rev. Earth Planet Sci.* 24, 191–224. doi:10.1146/annurev.earth.24.1.191

Eom, J., Yoshimura, T., Araoka, D., Gamo, T., and Kawahata, H. (2020). Magnesium isotopic composition of submarine vent fluids from arc and back-arc hydrothermal systems in the western Pacific. *Chem. Geol.* 551, 119767. doi:10.1016/j.chemgeo.2020.119767

Fruchter, N., Eisenhauer, A., Dietzel, M., Fietzke, J., Böhm, F., Montagna, P., et al. (2016). ^{88}Sr/^{86}Sr fractionation in inorganic aragonite and in corals. *Geochem. Cosmochim. Acta.* 178, 268–280. doi:10.1016/j.gca.2016.01.039

Gamo, T., Chiba, H., Fryer, P., Ishibashi, J., Ishii, T., Johnson, L. E., et al. (1994). Mariana 1992 diving surveys by Shinkai 6500 (Y9204 cruise): revisits to the mid-Mariana Trough hydrothermal area and discovery of hydrothermal vents in the southern Mariana region. *Proc. JAMSTEC Symp. Deep Sea Res.* 10, 153–162.

Gamo, T., Sakai, H., Kim, E.-S., Shitashima, K., and Ishibashi, J.-i. (1991). High alkalinity due to sulfate reduction in the CLAM hydrothermal field, Okinawa Trough. *Earth Planet Sci. Lett.* 107 (2), 328–338. doi:10.1016/0012-821x(91)90080-2

Gamo, T., Tsunogai, U., Ishibashi, J., Masuda, H., and Chiba, H. (1997). Chemical characteristics of hydrothermal fluids from the Mariana Trough. *Jamstec J. Deep Sea Res.*, 69–74

Grimaud, D., Ishibashi, J.-I., Lagabrielle, Y., Auzende, J.-M., and Urabe, T. (1991). Chemistry of hydrothermal fluids from the 17S active site on the north Fiji basin ridge (SW pacific). *Chem. Geol.* 93 (3-4), 209–218. doi:10.1016/0009-2541(91)90114-7

Halbach, P., Nakamura, K.-I., Wahsner, M., Lange, J., Sakai, H., Käselitz, L., et al. (1989). Probable modern analogue of Kuroko-type massive sulphide deposits in the Okinawa Trough back-arc basin. *Nature* 338 (6215), 496–499. doi:10.1038/338496a0

Halicz, L., Segal, I., Fruchter, N., Stein, M., and Lazar, B. (2008). Strontium stable isotopes fractionate in the soil environments?. *Earth Planet Sci. Lett.* 272 (1-2), 406–411. doi:10.1016/j.epsl.2008.05.005

Hardie, L. A. (1996). Secular variation in seawater chemistry: an explanation for the coupled secular variation in the mineralogies of marine limestones and potash evaporites over the past 600 m.y. *Geol.* 24 (3), 279–283. doi:10.1130/0091-7613(1996)024<0279:svisca>2.3.co;2

Hodell, D. A., Mead, G. A., and Mueller, P. A. (1990). Variation in the strontium isotopic composition of seawater (8 Ma to present): implications for chemical weathering rates and dissolved fluxes to the oceans. *Chem. Geol. Isot. Geosci.* 80 (4), 291–307. doi:10.1016/0168-9622(90)90011-z

Ishibashi, J. (1994). Chemical composition of hydrothermal fluids from the Suiyo and the mokuyo seamounts, Izu-Bonin Arc. *JAMSTEC Deep Sea Res.* 10, 89–97.

Ishibashi, J.-I., Grimaud, D., Nojiri, Y., Auzende, J.-M., and Urabe, T. (1994a). Fluctuation of chemical compositions of the phase-separated hydrothermal fluid from the North Fiji Basin Ridge. *Mar. Geol.* 116 (1-2), 215–226. doi:10.1016/0025-3227(94)90177-5

Ishibashi, J.-I. and Urabe, T. (1995). Hydrothermal activity related to arc-backarc magmatism in the western pacific, in *Backarc basins*. Editor B. Taylor (Boston, MA: Springer), 451–495. doi:10.1007/978-1-4615-1843-3_13

Ishibashi, J.-I., Wakita, H., Nojiri, Y., Grimaud, D., Jean-Baptiste, P., Gamo, T., et al. (1994b). Helium and carbon geochemistry of hydrothermal fluids from the North Fiji Basin spreading ridge (southwest Pacific). *Earth Planet Sci. Lett.* 128 (3-4), 183–197. doi:10.1016/0012-821x(94)90144-9

Ishibashi, J., Sano, Y., Wakita, H., Gamo, T., Tsutsumi, M., and Sakai, H. (1995). Helium and carbon geochemistry of hydrothermal fluids from the mid-Okinawa Trough back arc basin, southwest of Japan. *Chem. Geol.* 123 (1–4), 1–15. doi:10.1016/0009-2541(95)00051-m

Izawa, E., Motomura, Y., Tanaka, T., and Kimura, M. (1991). Hydrothermal carbonate chimneys in the Iheya Ridge of the Okinawa Trough. *JAMSTEC Deep Sea Res.* 7, 185–192.

Kawagucci, S., Ueno, Y., Takai, K., Toki, T., Ito, M., Inoue, K., et al. (2013). Geochemical origin of hydrothermal fluid methane in sediment-associated fields and its relevance to the geographical distribution of whole hydrothermal circulation. *Chem. Geol.* 339, 213–225. doi:10.1016/j.chemgeo.2012.05.003

Krabbenhöft, A., Eisenhauer, A., Böhm, F., Vollstaedt, H., Fietzke, J., Liebetrau, V., et al. (2010). Constraining the marine strontium budget with natural strontium isotope fractionations (^{87}Sr/^{86}Sr*, δ^{88}/^{86}Sr) of carbonates, hydrothermal solutions and river waters. *Geochem. Cosmochim. Acta.*, 74 (14), 4097–4109. doi:10.1016/j.gca.2010.04.009

Krabbenhöft, A., Fietzke, J., Eisenhauer, A., Liebetrau, V., Böhm, F., and Vollstaedt, H. (2009). Determination of radiogenic and stable strontium isotope ratios (^{87}Sr/^{86}Sr; δ^{88}/^{86}Sr) by thermal ionization mass spectrometry applying an ^{87}Sr/^{84}Sr double spike. *J. Anal. At. Spectrom.* 24, 1267–1271. doi:10.1039/b906292k

Lisitsyn, A. P., Crook, K. A. W., Bogdanov, Y. A., Zonenshayn, L. P., Murav'yev, K. G., Tufar, W., et al. (1993). A hydrothermal field in the rift zone of the Manus Basin, Bismarck Sea. *Int. Geol. Rev.* 35 (2), 105–126. doi:10.1080/00206819309465517

Liu, H.-C., You, C.-F., Zhou, H., Huang, K.-F., Chung, C.-H., Huang, W.-J., et al. (2017). Effect of calcite precipitation on stable strontium isotopic compositions: insights from riverine and pool waters in a karst cave. *Chem. Geol.* 456, 85–97. doi:10.1016/j.chemgeo.2017.03.008

McArthur, J. M., Howarth, R. J., and Bailey, T. R. (2001). Strontium isotope stratigraphy: LOWESS version 3: best fit to the marine Sr-isotope curve for 0-509 Ma and accompanying look-up table for deriving numerical age. *J. Geol.* 109 (2), 155–170. doi:10.1086/319243

Moynier, F., Agranier, A., Hezel, D. C., and Bouvier, A. (2010). Sr stable isotope composition of Earth, the Moon, Mars, Vesta and meteorites. *Earth Planet Sci. Lett.* 300 (3–4), 359–366. doi:10.1016/j.epsl.2010.10.017

Nakamura, K., and Takai, K.(2015). Geochemical constraints on potential biomass sustained by subseafloor water-rock interactions, in *Subseafloor biosphere linked to hydrothermal systems*. Editor M. Sunamura (Tokyo, Japan: Springer), 11–30. doi:10.1007/978-4-431-54865-2_2

Neymark, L. A., Premo, W. R., Mel'nikov, N. N., and Emsbo, P. (2014). Precise determination of δ^{88}Sr in rocks, minerals, and waters by double-spike TIMS: a powerful tool in the study of geological, hydrological and biological processes. *J. Anal. At. Spectrom.* 29 (1), 65–75. doi:10.1039/c3ja50310k

Noguchi, T., Shinjo, R., Ito, M., Takada, J., and Oomori, T. (2009). Barite geochemistry from hydrothermal chimneys of the Okinawa Trough: insight into chimney formation and fluid/sediment interaction. *J. Mineral. Petrol. Sci.* 106 (1), 26–35. doi:10.2465/jmps.090825

Nohara, M., Hirose, K., Eissen, J. P., Urabe, T., and Joshima, M. (1994). The North Fiji Basin basalts and their magma sources: Part II. Sr-Nd isotopic and trace element constraints. *Mar. Geol.* 116 (1–2), 179–195. doi:10.1016/0025-3227(94)90175-9

Ohno, T., and Hirata, T. (2007). Simultaneous determination of mass-dependent isotopic fractionation and radiogenic isotope variation of strontium in geochemical samples by multiple collector-ICP-mass spectrometry. *Anal. Sci.* 23 (11), 1275–1280. doi:10.2116/analsci.23.1275

Ohno, T., Komiya, T., Ueno, Y., Hirata, T., and Maruyama, S. (2008). Determination of ^{88}Sr/^{86}Sr mass-dependent isotopic fractionation and radiogenic isotope variation of ^{87}Sr/^{86}Sr in the Neoproterozoic Doushantuo Formation. *Gondwana Res.* 14 (1–2), 126–133. doi:10.1016/j.gr.2007.10.007

Pearce, C. R., Parkinson, I. J., Gaillardet, J., Charlier, B. L. A., Mokadem, F., and Burton, K. W. (2015a). Reassessing the stable (δ^{88}/^{86}Sr) and radiogenic (^{87}Sr/^{86}Sr) strontium isotopic composition of marine inputs. *Geochem. Cosmochim. Acta.* 157, 125–146. doi:10.1016/j.gca.2015.02.029

Pearce, C. R., Parkinson, I. J., Gaillardet, J., Chetelat, B., and Burton, K. W. (2015b). Characterising the stable (δ^{88}/^{86}Sr) and radiogenic (^{87}Sr/^{86}Sr) isotopic composition of strontium in rainwater. *Chem. Geol.* 409, 54–60. doi:10.1016/j.chemgeo.2015.05.010

Raddatz, J., Liebetrau, V., Rüggeberg, A., Hathorne, E., Krabbenhöft, A., Eisenhauer, A., et al. (2013). Stable Sr-isotope, Sr/Ca, Mg/Ca, Li/Ca and Mg/Li ratios in the scleractinian cold-water coral Lophelia pertusa. *Chem. Geol.* 352, 143–152. doi:10.1016/j.chemgeo.2013.06.013

Raymo, M. E., and Ruddiman, W. F. (1992). Tectonic forcing of late Cenozoic climate. *Nature* 359 (6391), 117. doi:10.1038/359117a0

Rimstidt, J. D., Balog, A., and Webb, J. (1998). Distribution of trace elements between carbonate minerals and aqueous solutions. *Geochem. Cosmochim. Acta.* 62 (11), 1851–1863. doi:10.1016/s0016-7037(98)00125-2

Rüggeberg, A., Fietzke, J., Liebetrau, V., Eisenhauer, A., Dullo, W. C., and Freiwald, A. (2008). Stable strontium isotopes (δ^{88}/^{86}Sr) in cold-water corals–a new proxy for reconstruction of intermediate ocean water temperatures. *Earth Planet Sci. Lett.* 269 (3–4), 570–575. doi:10.1016/j.epsl.2008.03.002

Sakai, H., Gamo, T., Kim, E.-S., Shitashima, K., Yanagisawa, F., Tsutsumi, M., et al. (1990). Unique chemistry of the hydrothermal solution in the mid-Okinawa Trough Backarc Basin. *Geophys. Res. Lett.* 17 (12), 2133–2136. doi:10.1029/gl017i012p02133

Naganuma, H., Gamo, T., Kim, E.-S., Tsutsumi, M., Tanaka, T., Ishibashi, J., et al. (1990b). Venting of carbon dioxide-rich fluid and hydrate formation in mid-Okinawa trough backarc basin. *Science* 248 (4959), 1093–1096. doi:10.1126/science.248.4959.1093

Shalev, N., Gavrieli, I., Halicz, L., Sandler, A., Stein, M., and Lazar, B. (2017). Enrichment of 88 Sr in continental waters due to calcium carbonate precipitation. *Earth Planet Sci. Lett.* 459, 381–393. doi:10.1016/j.epsl.2016.11.042

Sibuet, J.-C., Hsu, S.-K., Shyu, C.-T., and Liu, C.-S. (1995). Structural and kinematic evolutions of the Okinawa Trough backarc basin, in *Backarc basins*, Editor B. Taylor (Boston, MA: Springer), 343–379. doi:10.1007/978-1-4615-1843-3_9

Stevenson, E. I., Aciego, S. M., Chutcharavan, P., Parkinson, I. J., Burton, K. W., Blakowski, M. A., et al. (2016). Insights into combined radiogenic and stable strontium isotopes as tracers for weathering processes in subglacial environments. *Chem. Geol.* 429, 33–43. doi:10.1016/j.chemgeo.2016.03.008

Stevenson, E. I., Hermoso, M., Rickaby, R. E. M., Tyler, J. J., Minoletti, F., Parkinson, I. J., et al. (2014). Controls on stable strontium isotope fractionation in coccolithophores with implications for the marine Sr cycle. *Geochem. Cosmochim. Acta.* 128, 225–235. doi:10.1016/j.gca.2013.11.043

Tsuji, T., Takai, K., Oiwane, H., Nakamura, Y., Masaki, Y., Kumagai, H., et al. (2012). Hydrothermal fluid flow system around the Iheya North Knoll in the mid-Okinawa trough based on seismic reflection data. *J. Volcanol. Geoth. Res.* 213–214, 41–50. doi:10.1016/j.jvolgeores.2011.11.007

Tsunogai, U., Ishibashi, J., Wakita, H., Gamo, T., Watanabe, K., Kajimura, T., et al. (1994). Peculiar features of Suiyo Seamount hydrothermal fluids, Izu-Bonin Arc: differences from subaerial volcanism. *Earth Planet Sci. Lett.* 126 (4), 289–301. doi:10.1016/0012-821x(94)90113-9

Veizer, J., Ala, D., Azmy, K., Bruckschen, P., Buhl, D., Bruhn, F., et al. (1999). ^{87}Sr/^{86}Sr, δ^{13}C and δ^{18}O evolution of Phanerozoic seawater. *Chem. Geol.* 161 (1–3), 59–88. doi:10.1016/s0009-2541(99)00081-9

Voigt, J., Hathorne, E. C., Frank, M., Vollstaedt, H., and Eisenhauer, A. (2015). Variability of carbonate diagenesis in equatorial Pacific sediments deduced from radiogenic and stable Sr isotopes. *Geochem. Cosmochim. Acta.* 148, 360–377. doi:10.1016/j.gca.2014.10.001

Voigt, M., Pearce, C. R., Baldermann, A., and Oelkers, E. H. (2018). Stable and radiogenic strontium isotope fractionation during hydrothermal seawater-basalt interaction. *Geochem. Cosmochim. Acta.* 240, 131–151. doi:10.1016/j.gca.2018.08.018

Vollstaedt, H., Eisenhauer, A., Wallmann, K., Böhm, F., Fietzke, J., Liebetrau, V., et al. (2014). The Phanerozoic δ^{88}/^{86}Sr record of seawater: new constraints on past changes in oceanic carbonate fluxes. *Geochem. Cosmochim. Acta*, 128, 249–265. doi:10.1016/j.gca.2013.10.006

Volpe, A. M., Macdougall, J. D., and Hawkins, J. W. (1987). Mariana trough basalts (MTB): trace element and SrNd isotopic evidence for mixing between MORB-like and Arc-like melts. *Earth Planet Sci. Lett.* 82 (3-4), 241–254. doi:10.1016/0012-821x(87)90199-3

Von Damm, K. L. and Bischoff, J. L. (1987). Chemistry of hydrothermal solutions from the southern Juan de Fuca Ridge. *J. Geophys. Res.* 92 (B11), 11334–11346. doi:10.1029/jb092ib11p11334

Von Damm, K. L., Edmond, J. M., Measures, C. I., and Grant, B. (1985). Chemistry of submarine hydrothermal solutions at guaymas basin, gulf of California. *Geochem. Cosmochim. Acta.* 49 (11), 2221–2237. doi:10.1016/0016-7037(85)90223-6

Wakaki, S., Obata, H., Tazoe, H., and Ishikawa, T. (2017). Precise and accurate analysis of deep and surface seawater Sr stable isotopic composition by double-spike thermal ionization mass spectrometry. *Geochem. J.* 51 (3), 227–239. doi:10.2343/geochemj.2.0461

Wei, G., Ma, J., Liu, Y., Xie, L., Lu, W., Deng, W., et al. (2013). Seasonal changes in the radiogenic and stable strontium isotopic composition of Xijiang River water: implications for chemical weathering. *Chem. Geol.* 343, 67–75. doi:10.1016/j.chemgeo.2013.02.004

Yamaoka, K., Hong, E., Ishikawa, T., Gamo, T., and Kawahata, H. (2015). Boron isotope geochemistry of vent fluids from arc/back-arc seafloor hydrothermal systems in the western Pacific. *Chem. Geol.* 392, 9–18. doi:10.1016/j.chemgeo.2014.11.009

You, C. F., Butterfield, D. A., Spivack, A. J., Gieskes, J. M., Gamo, T., and Campbell, A. J. (1994). Boron and halide systematics in submarine hydrothermal systems: effects of phase separation and sedimentary contributions. *Earth Planet Sci. Lett.* 123 (1–3), 227–238. doi:10.1016/0012-821x(94)90270-4

Conflict of Interest: The authors declare that the research was conducted in the absence of any commercial or financial relationships that could be construed as a potential conflict of interest.